Deprotonation-Induced Enantioselective Aggregation and Deprotonation-Induced Ligand Rearrangement of Copper(II) Complexes Yield 1D Homochiral and Heterochiral Chains and a Cyclic Tetramer, Respectively

Yoshiki Shii,[†] Yuri Motoda,[†] Toshihiro Matsuo,[†] Fumiaki Kai,[†] Toshio Nakashima,[‡] Jean-Pierre Tuchagues,[§] and Naohide Matsumoto*,[†]

Department of Chemistry, Faculty of Science, Kumamoto University, Kurokami 2-39-1, Kumamoto 860-8555, Japan, Faculty of Education, Oita University, Dan-noharu 700, Oita 870-1192, Japan, and Laboratoire de Chimie de Coordination, CNRS, UPR 8241, 205 route de Narbonne, 31077 Toulouse Cédex, France

Received November 17, 1998

The copper(II) complexes of protonated pentadentate Schiff-base ligands with $[Cu(H_2L^n)](ClO_4)_2$ formula (n = 3−6, **3**−**6**) have been synthesized and characterized (H_2L^3 = *N*-((2-methylimidazol-4-yl)methylene)-3-aminpropyl-*N*′-((2-methylimidazol-4-yl)methylene)-4′-aminobutylamine, H_2L^4 = *N*-((2-phenylimidazol-4-yl)methylene)-3-aminpropyl-*N*′-((2-phenyl-imidazol-4-yl)methylene)-4′-aminobutylamine, H_2L^5 = *N*,*N*′-bis((2-phenylimidazol-4-yl)methylene)-3,3′-diaminodipropylmethylamine, H_2L^6 = *N*-((2-methylimidazol-4-yl)methylene)-2-aminoethyl-*N*′-((2-methylimidazol-4-yl)methylene)-3′-aminopropylamine. The mono-deprotonated complexes **3**′, **4**′, and **5**′ contain one imidazole and one imidazolate groups per unit and are Δ (clockwise) or Λ (anticlockwise) enantiomorphs due to the spiral arrangement of the ligand around copper(II) ion. They function as chiral building components for a self-assembly process resulting from the formation of hydrogen bonds between the imidazole and imidazolate groups of adjacent units to yield 1D zigzag-chain structures. The distance between hydrogen-bonded nitrogen atoms is 2.81(2), 2.832(9), and 2.875(9) Å for **3**′, **4**′, and **5**′, respectively. The crystal lattice of **3**′ yielded either ...ΔΔΔ... or ...ΛΛΛ... isotactic 1D zigzag-chains, while the crystal lattices of **4**′ and **5**′ yielded ...ΔΛΔΛ... syndiotactic 1D zigzag-chains. In **3**′, two adjacent methyl groups at the 2-position connected by hydrogen bond array in the same direction, thus allowing homochiral aggregation of the complex molecules in a 1D chain. On the other hand, in **4**′ and **5**′, two adjacent bulky phenyl groups require opposite orientations, thus allowing heterochiral aggregation. Enantioselective aggregation with homochirality or heterochirality can thus be controlled with suitable substituents. While its mononuclear precursor **6** is pentacoordinated with the N_5 donor set of the pentadentate ligand H_2L^6, the deprotonated complex **6**′ has an imidazolate-bridged tetranuclear cyclic structure with a Cu−Cu distance of 6.086(2) Å. The ligand in **6**′ is tetradentate and includes an hexahydropyrimidine ring resulting from a deprotonation induced rearrangement reaction.

Introduction

Self-assembly and self-organization are the keys to the areas of supramolecular chemistry and crystal engineering.[1,2] The directed manipulation of intermolecular interactions (coordination bond, hydrogen bond, $\pi-\pi$ interaction, etc.) give supramolecular assemblies through the design of instructed monomeric and polymeric species.[3,4]

Chirality has been one of the most important subjects in science and the detailed insight into the mechanism of enantioselectivity is essential, because asymmetric synthesis and optical resolution are not only fundamental in chemistry but also practically important in pharmacology and industry.[5] Chirality

* To whom correspondence should be addressed. Tel./Fax: +81-96-342-3390. E-mail: naohide@aster.sci.kumamoto-u.ac.jp.
[†] Kumamoto University.
[‡] Oita University.
[§] Laboratoire de Chimie de Coorrdination du CNRS.

(1) (a) Lehn, J.-M. *Supramolecular Chemistry*; VCH: Weinheim, Germany, 1995. (b) *Transition Metals in Supramolecular Chemistry*; Fabbrizzi, L., Poggi, A., Eds.; ASI Kluwer Academic Publisheres: Dordrecht, The Netherlands, 1994. (c) Vogtle, V. *Supramolecular Chemistry*; Wiley: New York, 1991. (d) Stang, P. J.; Olenyuk, B. *Angew. Chem., Int. Ed. Engl.* **1996**, *35*, 732. (e) Constable, E. C. *Nature* **1990**, *346*, 314. (f) Goodgame, D. M. L.; Williams, D. J.; Winpenny, R. E. P. *J. Chem. Soc., Dalton Trans.* **1991**, 917. (g) Carina, R. F.; Bernardinelli, G.; Williams, A. F. *Angew. Chem., Int. Ed. Engl.* **1993**, *32*, 1463. (h) Ashton, P. R.; Philip, D.; Spencer, N.; Stoddart, J. F. *J. Chem. Soc., Chem. Commun.* **1992**, 1124.

(2) (a) Kahn, O. *Molecular Magnetism*; VCH: Weinheim, Germany, 1993. (b) Kahn, O. *Structure and Bonding*; Springer-Verlag: Berlin, Germany, 1987 Vol. 68. (c) Miller, J. S.; Epstein, A. J.; Reiff, W. M. *Chem. Rev.* **1988**, *88*, 201. (d) Miyasaka, H.; Matsumoto, N.; Okawa, H.; Re, N.; Gallo, E.; Floriani, C. *J. Am. Chem. Soc.* **1996**, *118*, 981.

(3) See, for examples: (a) Constable, E. C. *Tetrahedron.* **1992**, *48*, 10013. (b) Potts, K. T.; Keshavarz-K, M.; Tham, F. S.; Abruña, H. D.; Arana, C. *Inorg. Chem.* **1993**, *32*, 4436. (c) Krämer, R.; Lehn, J.-M.; De Cian, A.; Fischer, F. *Angew. Chem., Int. Ed. Engl.* **1993**, *32*, 703. (d) Gelling, O. J.; Bolhuis, F. V.; Feringa, B. L. *J. Chem. Soc., Chem. Commun.* **1991**, 917. (e) Tadokoro, M.; Daigo, M.; Isobe, K.; Matsumoto, K.; Nakasuji, K. *Mol. Cryst. Liq. Cryst.* **1997**, *306*, 391. (f) Tadokoro, M.; Isobe, K.; Uekusa, H.; Ohashi, Y.; Toyota, J.; Tashiro, K.; Nakasuji, K. *Angew. Chem., Int. Ed.* **1999**, *38*, 95.

(4) See, for examples: (a) Abrahams, B. F.; Hoskins, B. F.; Michail, D. M.; Robson, R. *Nature* **1994**, *369*, 727. (b) Fujita, F.; Kwon, Y.; Sasaki, O.; Yamaguchi, K.; Ogura, K. *J. Am. Chem. Soc.* **1995**, *117*, 7287. (c) Kawata, S.; Kitagawa, S.; Kumagai, H.; Kudo, C.; Kamesaki, H.; Ishiyama, T.; Suzuki, R.; Kondo, M.; Katada, M. *Inorg. Chem.* **1996**, *35*, 4449. (d) Yaghi, O. M.; Li, G.; Li, H. *Nature* **1995**, *378*, 703. (e) Carlucci, L.; Ciani, G.; Proserpio, D. M.; Sironi, A. *J. Am. Chem. Soc.* **1995**, *117*, 4562.

10.1021/ic9813260 CCC: $18.00
Published on Web 07/09/1999

Chart 1. Structure and Abbreviations of the Complexes

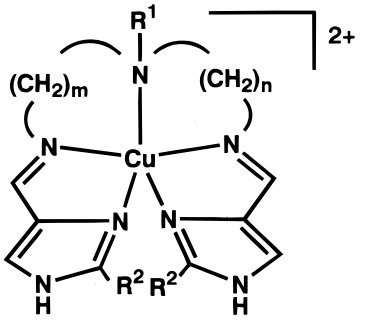

	Complex	(m, n, R^1, R^2)	ref.
1	$[Cu(H_2L^1)](ClO_4)_2$	(3, 3, H, H)	6
2	$[Cu(H_2L^2)](ClO_4)_2$	(3, 3, H, Me)	6
3	$[Cu(H_2L^3)](ClO_4)_2$	(3, 4, H, Me)	*
4	$[Cu(H_2L^4)](ClO_4)_2$	(3, 4, H, Ph)	*
5	$[Cu(H_2L^5)](ClO_4)_2$	(3, 3, Me, Ph)	*
6	$[Cu(H_2L^6)](ClO_4)_2$	(2, 3, H, Me)	*

* this work

is expressed on both the molecular and supramolecular levels, and supramolecular chirality results not only from the properties of the components, but also from the way in which they associate. Although spontaneous resolution through chiral selection in molecular recognition directed self-assembly have been the leading process in the organization of basic materials giving rise to primitive living organisms, very little attention has been yet paid to the profound influence of chirality upon the superstructures. Along this line, the use of self-complementary (*plerotopic*) double-faced H-bonding recognition units (*Janus* molecules) are capable of undergoing not only homo-self-assembly into polymeric entities, but also self-resolution, which results in the formation of homochiral supramolecular entities from racemic components, as pointed out by Lehn.[1a]

In a recent paper[6] of our studies on metal complexes involving imidazole groups,[7] we have reported copper(II) complexes exhibiting a self-complementary (*plerotopic*) double-faced H-bonding recognition and enantioselective self-assembly behavior. The schematic structure of the copper(II) complexes, $[Cu(H_2L^1)](ClO_4)_2$ (**1**) and $[Cu(H_2L^2)](ClO_4)_2$ (**2**), are given in Chart 1. The mono-deprotonated complexes, $[Cu(HL^1)]ClO_4$ (**1′**) and $[Cu(HL^2)]ClO_4$ (**2′**), include one imidazole and one imidazolate moiety, and due to the spiral arrangement of the acyclic ligand, Δ (clockwise) and Λ (anticlockwise) enantiomers are present in equal proportions (Scheme 1). These mono-positive complex cation functions as chiral building components and aggregate into evenly distributed ...ΔΔΔ... and ...ΛΛΛ... homochiral 1D zigzag-chains, owing to hydrogen-bonding between the imidazole and imidazolate groups of adjacent homochiral units (Scheme 2).

Scheme 1. Δ (Clockwise) and Λ (Anticlockwise) Enantiomorphs Due to the Spiral Arrangement of Pentadentate Ligand

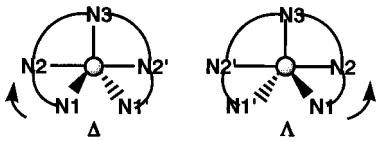

Scheme 2 1D Zigzag-Chain Due To Hydrogen-Bonding between the Imidazole and Imidazolate Groups of Adjacent Units

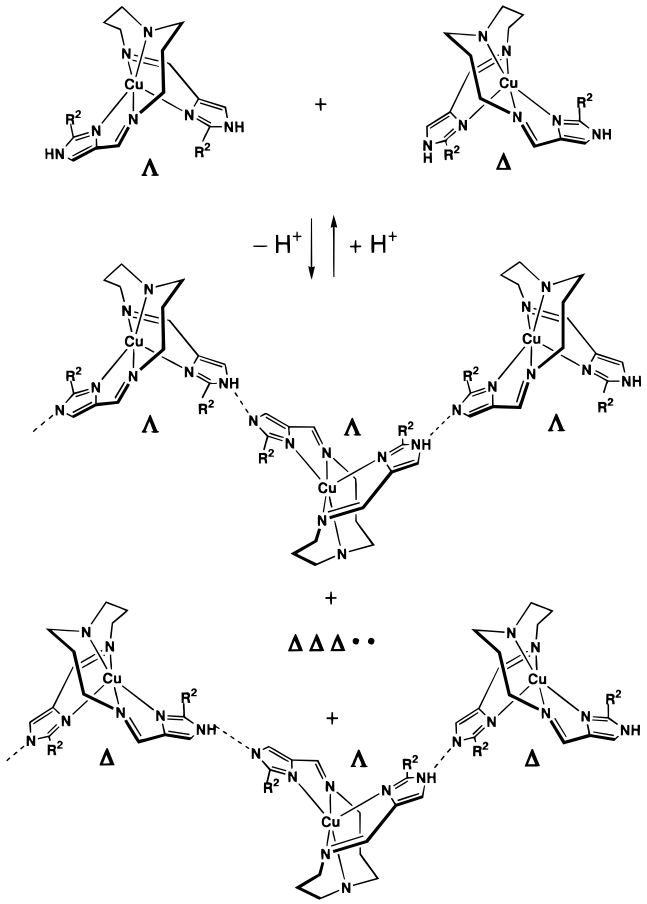

If 1D enantioselective homochiral aggregation was extended to 3-D system, a self-resolution will be achieved in crystal. For this purpose, it is necessary to verify the factors controlling enantioselectivity. To get the detailed insight, in this study we have investigated a series of copper(II) complexes with analogous H_2L^n pentadentate ligands, $[Cu(H_2L^n)](ClO_4)_2$ formula (n = 3−6, **3**−**6**), where the 2-substituted imidazole moiety, the lengths of the $-(CH_2)_n-$ fragments in the triamine moiety, and the nature of the central amine were modified. The schematic structures of the complexes are given in Chart 1 and the ligands are the 2:1 condensation products of 2-methyl (or 2-phenyl)-4-formylimidazole and linear triamines: H_2L^3 = *N*-((2-methylimidazol-4-yl)methylene)-3-aminpropyl-*N*′-((2-methylimidazol-

(5) (a) Jacques, J. J.; Collet, A.; Wilen, S. H. *Enantiomers, Racemates and Resolutions*; Kringer: Malabar, FL, 1991. (b) Cray, D. P.; Mellor, D. P. *Top. Curr. Chem.* **1976**, 63, 1. (c) Lehn, J.-M. *Supramolecular Chemistry*; VCH: Weinheim, Germany, 1995; Section 9.7.

(6) Miyasaka, H.; Okamura, S.; Nakashima, T.; Matsumoto, N. *Inorg. Chem.* **1997**, *36*, 4329.

(7) (a) Matsumoto, N.; Mizuguchi, Y.; Mago, G.; Eguchi, S.; Miyasaka, H.; Nakashima, T.; Tuchagues, J.-P. *Angew. Chem., Int. Ed. Engl.* **1997**, *36*, 1860. (b) Nozaki, T.; Ushio, H.; Mago, G.; Matsumoto, N.; Okawa, H.; Yamakawa, Y.; Anno, T.; Nakashima, T. *J. Chem. Soc., Dalton Trans.* **1994**, 2339. (c) Matsumoto, N.; Ohba, M.; Mitsumi, M.; Inoue, K.; Hashimoto, Y.; Okawa, H. *Mol. Cryst. Liq. Cryst.* **1993**, *233*, 299. (d) Matsumoto, N.; Akui, T.; Murakami, H.; Kanesaka, J.; Ohyoshi, A.; Okawa, H. *J. Chem. Soc., Dalton Trans.* **1988**, 1021. (e) Matsumoto, N.; Nozaki, T.; Ushio, H.; Motoda, K.; Ohba, M.; Mago, G.; Okawa, H. *J. Chem. Soc., Dalton Trans.* **1993**, 2157. (f) Matsumoto, N.; Mimura, M.; Sunatsuki, Y.; Eguchi, S.; Mizuguchi, Y.; Miyasaka, H.; Nakashima, T. *Bull. Chem. Soc. Jpn.* **1997**, *70*, 2461.

4-yl)methylene)-4′-aminobutylamine, H_2L^4 = *N*-((2-phenylimidazol-4-yl)methylene)-3-aminpropyl-*N*′-((2-phenyl-imidazol-4-yl)-methylene)-4′-aminobutylamine, H_2L^5 = *N*,*N*′-bis((2-phenyl-imidazol-4-yl)methylene)-3,3′-diaminodipropylmethylamine, H_2L^6 = *N*-((2-methylimidazol-4-yl)methylene)-2-aminoethyl-*N*′-((2-methylimidazol-4-yl)methylene)-3′-aminopropylamine. The effect of the 2-substituted imidazole moiety on the homochiral and heterochiral aggregation was investigated. In addition to that, the effects of the length of the -$(CH_2)_n$- fragments in the triamine moiety, or/and the nature of the central amine function was investigated. The synthesis, characterization, structure, and pH-dependent behavior of the four protonated mononuclear precursors **3**−**6** and the four related supramolecular structures (**3′**−**6′**) resulting from their deprotonation-promoted self-assembly are reported in this contribution.

Results and Discussion

Synthesis and Characterization of the Protonated Complexes 3−**6.** The pentadentate Schiff-base ligands H_2L^n (n = 3−6) were prepared through 2:1 condensation reactions between 2-methyl(or 2-phenyl)-4-formylimidazole and either of the three linear triamines, *N*-(3-aminopropyl)-1,4-butanediamine), *N*,*N*′-bis(3-aminopropyl)methylamine, and (*N*-(2-aminoethyl)-1,3-propanediamine in methanol. Each ligand reaction mixture was subsequently used for the synthesis of the corresponding copper(II) complex without isolation of the ligand. The C, H, and N microanalyses of the copper(II) complexes agree well with $[Cu(H_2L^n)](ClO_4)_2 \cdot xH_2O$ chemical formula (x = 0 for **3**, **4**, and **6**; x = 0.5 for **5**). The infrared spectra show the characteristic absorption bands attributable to the imidazole ν_{N-H} (3150−3300 cm^{-1}), Schiff-base $\nu_{C=N}$ (1600−1640 cm^{-1}), and perchlorate ν_{Cl-O} (1080−1180 cm^{-1}) moieties.[8] The molar electrical conductivities of **3**, **5**, and **6** in 10^{-3} M aqueous solutions (200, 187, and 203 S cm^2 mol^{-1}, respectively) are in the expected range for 1:2 electrolytes in H_2O,[9] indicating that in aqueous solution these complexes involve two neutral imidazole moieties and uncoordinated perchlorate anions.

Synthesis and Characterization of the Deprotonated Complexes 3′−**5′.** The mono-deprotonated complexes **3′**, **4′**, and **5′** were obtained as well-grown green crystals when 2 equiv of triethylamine were added to the 1:1 mixed solution of the ligand and copper(II) perchlorate hexahydrate in methanol. The C, H, and N microanalyses agree well with the mono-deprotonated $[Cu(HL^n)]ClO_4 \cdot xH_2O$ formula (x = 0 for **3′**, 0.5 for **4′**, 1 for **5′**). The infrared spectra show the characteristic absorption bands attributable to the ν_{N-H}, $\nu_{C=N}$, and perchlorate moieties.[8] The molar electrical conductivity was not measured due to the sparing solubility of these complexes in common organic solvents and water. The effective magnetic moments per copper for **3′**−**5′**, μ_{eff}, are constant over the temperature range and the magnetic susceptibility obeys the Curie law. The 1.81 μ_B value of **4′** is compatible with the 1.73 μ_B spin-only value for $S = {}^1/_2$. These data indicate that **3′**−**5′** behave as a magnetically diluted $S = {}^1/_2$ spin system.

On the other hand, the complex resulting from deprotonation of **6** was obtained by a synthetic procedure different from those of **3′**−**5′**, as is described in the Experimental Section. Even when a large excess of triethylamine was added to a methanolic solution of **6**, no deprotonated complex could be isolated but **6** was recovered. However, on addition of 2 equiv of an aqueous NaOH solution to a 1:1:1 mixed-solution of the ligand, copper(II) chloride dihydrate, and sodium perchlorate, the deprotonated complex **6′** was obtained as well-grown green crystals. The C, H, and N microanalyses of the sample dried under reduced pressure agree well with the formula $[Cu_4(HL^{6'})_4](ClO_4)_4 \cdot H_2O$, although the X-ray analysis indicated that the crystal contains 16 crystal waters per tetranuclear molecule. The infrared spectrum shows the characteristic absorption bands attributable to the ν_{N-H}, $\nu_{C=N}$, and perchlorate moieties.[8] The molar electrical conductivity per Cu in water (100 S cm^2 mol^{-1}) is in the expected range for a 1:1 electrolyte.[9] The X-ray structural analysis of **6′** described hereafter showed an unexpected imidazolate-bridged tetranuclear cyclic structure in which the HL^6 ligand has rearranged upon deprotonation.

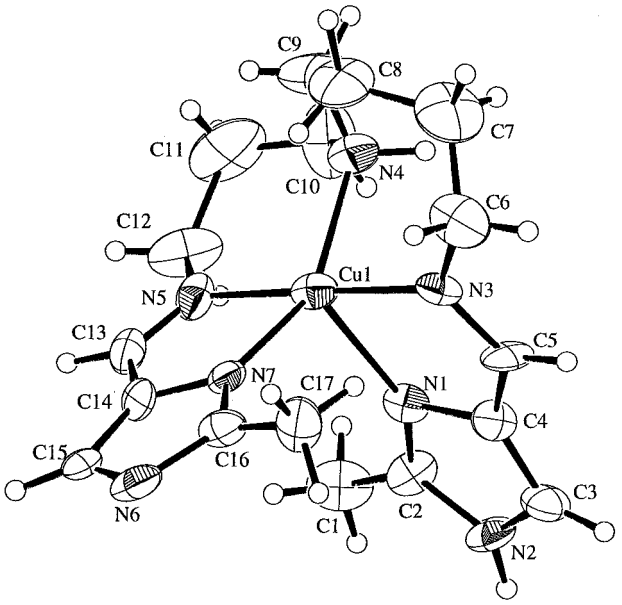

Figure 1. ORTEP drawing of the unique atoms of the cation (Δ enantiomorph) for **3′** with the atom numbering scheme, showing 30% probability ellipsoids.

Structural Description of 3′, 4′, and 5′. The crystals of the mono-deprotonated complexes **3′**, **4′**, and **5′** consist of mono-positive copper(II) complex cations and perchlorate counter-anions. One oxygen atom of perchlorate ion is weakly hydrogen-bonded to the central amine nitrogen with the N···O distances of 2.97(3) and 3.15(1) Å for **3′** and **4′**, respectively. The ORTEP drawings of the constitutive units in **3′** and **4′**, including atom numbering scheme are shown in Figures 1 and 2, respectively. ORTEP drawing of **5′** is deposited as Figure S1. Selected bond distances and angles with their estimated standard deviations are summarized in Table 1.

Each copper(II) ion of **3′**, **4′**, and **5′** assumes pentacoordination with the N_5 donor set including one imidazole, one imidazolate, two imine, and the central amino nitrogen atoms of the pentadentate ligand. The Cu−N bond distances are in the ranges of 2.00(1)−2.21(1) Å for **3′**, 1.995(6)−2.354(6) Å for **4′**, and 1.954(6)−2.396(6) Å for **5′**, respectively. The Cu−N distance for the protonated imidazole moiety, Cu−N(1), is substantially longer than that for the deprotonated imidazolate moiety, Cu−N(7): [Cu−N(1), Cu−N(7)] = [2.21(1), 2.04(1) Å], [2.354(6), 2.000(6) Å], and [2.396(6), 2.033(6) Å] for **3′**, **4′**, and **5′**, respectively.

One important structural feature is that the copper(II) complex cations are either Δ or Λ enantiomorphs due to the spiral arrangement of the acyclic pentadentate ligand around the N(3)−Cu−N(5) axis. The Δ and Λ enantiomorphs are defined as shown in Scheme 1: the front imidazole nitrogen atom is

(8) Nakamoto, K. *Infrared and Raman Spectra of Inorganic and Coordination Compounds*, 4th ed.; John Wiley & Sons: New York, 1986.
(9) Geary, E. *J. Coord. Chem. Rev.* **1971**, *7*, 81.

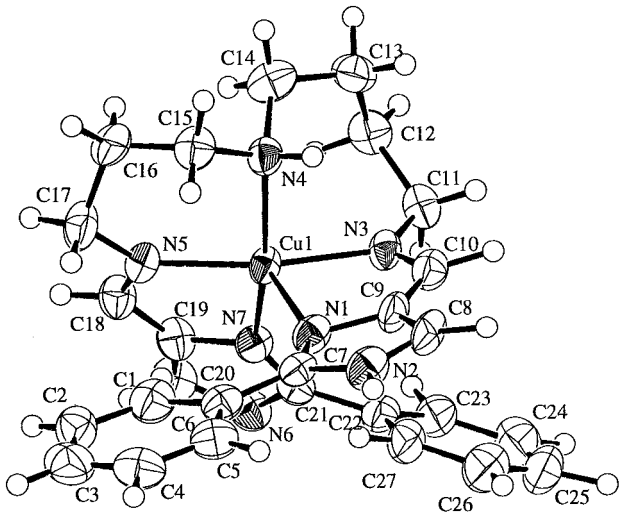

Figure 2. ORTEP drawing of the cation (Λ enantiomorph) of **4′** with the atom numbering scheme, showing 50% probability ellipsoids.

Table 1. Selected Bond Distances (Å) and Angles (deg) of **3′**, **4′**, and **5′**

	3′	**4′**	**5′**
	Bond Distances (Å)		
Cu−N(1)	2.21(1)	2.354(6)	2.396(6)
Cu−N(3)	2.02(1)	1.995(6)	1.954(6)
Cu−N(4)	2.04(2)	2.053(6)	2.084(6)
Cu−N(5)	2.00(1)	2.014(6)	1.987(6)
Cu−N(7)	2.04(1)	2.000(6)	2.033(6)
	Hydrogen Bond Distances (Å)[a]		
N(2)*···N(6)	2.81(2)[a]	2.832(9)[b]	2.875(9)[b]
	Bond Angles (deg)		
N(1)−Cu−N(3)	79.9(6)	78.9(2)	77.4(2)
N(1)−Cu−N(4)	107.0(6)	90.6(2)	104.9(2)
N(1)−Cu−N(5)	97.6(6)	113.9(2)	104.1(2)
N(1)−Cu−N(7)	102.9(5)	110.2(2)	93.0(2)
N(3)−Cu−N(4)	89.2(6)	86.4(2)	86.7(2)
N(3)−Cu−N(5)	177.5(6)	167.0(2)	176.0(3)
N(3)−Cu−N(7)	98.4(6)	95.9(2)	94.3(2)
N(4)−Cu−N(5)	91.0(6)	91.1(2)	96.5(3)
N(4)−Cu−N(7)	150.0(6)	159.2(2)	161.8(2)
N(5)−Cu−N(7)	82.7(6)	82.0(3)	81.9(3)

[a] Symmetry operations: (a) $^1/_2 + x$, $^1/_2 - y$, $-z$; (b) x, $^1/_2 - y$, $^1/_2 + z$.

defined as N1 against the back imidazole nitrogen N1′; the clockwise direction of the N1→N2→N3→N2′→N1′ spiral in the pentacoordinated ligand corresponds to the Δ enantiomorph, and the anticlockwise direction of the N1→N2→N3→N2′→N1′ spiral corresponds to the Λ enantiomorph.[10,11] As the deprotonated complexes **3′**−**5′** crystallize in the centrosymmetric space groups $P2_1/c$ or *Pbca*, the Δ and Λ enantiomorphs of the cationic complex coexist as racemic species in the crystals.

The imidazolate nitrogen atom N(6) of each copper(II) complex cation is hydrogen-bonded to the imidazole nitrogen atom N(2)* of an adjacent unit, yielding a one-dimensional zigzag-chain with intermolecular hydrogen-bond distances of 2.81(2), 2.832(9), and 2.875(9) Å for **3′**, **4′**, and **5′**, respectively. The 1D zigzag-chain structures for **3′**, **4′**, and **5′** (Figure 3) are thus made from plerotopic Janus complex cations.

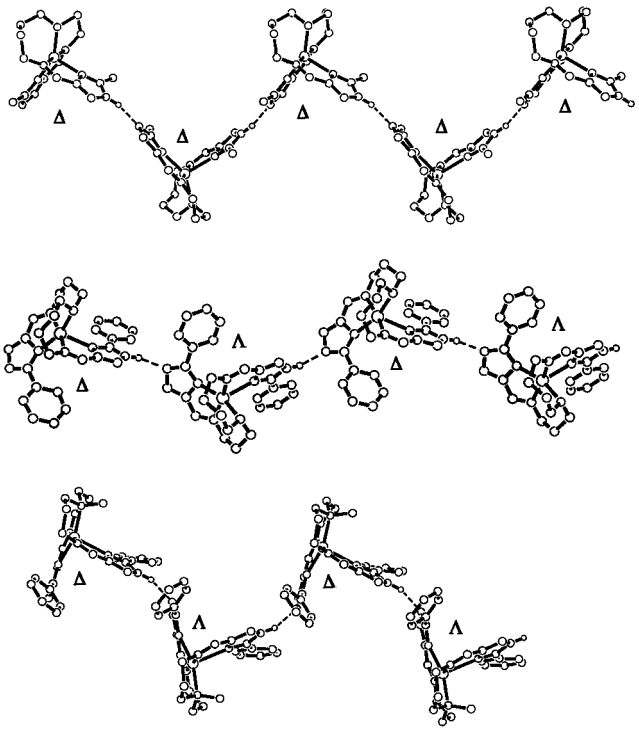

Figure 3. 1D zigzag-chain structure formed by hydrogen bonds of **3′** (top), **4′** (center), and **5′** (bottom). Within a zigzag-chain of **3′**, the same enantiomorphs are linked by the hydrogen bonds. Within a zigzag-chain of **4′** and **5′**, Δ and Λ enantiomorphs are arrayed alternately. The dashed line represents the hydrogen bonds.

Within a zigzag-chain of **3′** (*Pbca*) running along the *a*-axis, hydrogen-bonded complex cations are related by a 2-fold screw axis and the chirality of the complex cations is preserved in the zigzag-chain. The 1D zigzag-chains of **3′** are isotactic with respect to the Δ and Λ chirality of the complex cations: a Δ enantiomorph only aggregates with another Δ enantiomorph through a hydrogen bond and a Λ enantiomorph only aggregates with another Λ enantiomorph, yielding evenly distributed ...ΔΔΔ... and ...ΛΛΛ... 1D chains. Therefore, although homoself-assembly (implying self-resolution) is achieved, no net chirality is exhibited by the crystal itself.

On the other hand, in **4′** and **5′** ($P2_1/c$), the zigzag-chains run along the *c* axis and hydrogen-bonded complex cations are related by a *c* glide plane and complex cations with Δ and Λ opposite chiralities alternate along the chains, thus syndiotactic ...ΔΛΔΛ... 1D zigzag-chains of **4′** and **5′**.

Steric Effect of the Substituent on Enantioselective Aggregation. Although the steric effect on enantioselective crystallization of $[Co(en)_2XY]Z$ and the analogous compounds has already explored and reported,[12] a more simple relation can be drawn in this molecular system. The only difference in the ligand framework of **3′** and **4′** is the 2-substituent of the imidazole moieties: a methyl group for **3′**, and a phenyl group for **4′**. Figure 4a and b show the CHARON drawings and space filling representation of two hydrogen-bonded complex cations in **3′** and in **4′**, respectively.

The phenyl groups of adjacent complex cations in **4′** need to be oriented in opposite directions, to avoid steric hindrance while allowing for the formation of a 1D hydrogen bonded chain-structure, as evidenced by the space filling representation. Then

(10) *Nomenclature of Inorganic Chemistry: Recommendations*; Blackwell: Oxford, U.K., 1990.

(11) In ref 10, the symbol of chirality used for these complexes is *C* (clockwise) and *A* (anticlockwise) instead of Δ and Λ. In this paper, the symbols Δ and Λ are used to describe the chirality for the reported complexes.

(12) (a) Cai, J.; Myrczek, J.; Bernal, I. *J. Chem. Soc., Dalton Trans.* **1995**, 611. (b) Bernal, I. Cai, J.; Myrczek, J. *Acta Chim. Hungaria—Models Chem.* **1993**, *130*, 555.

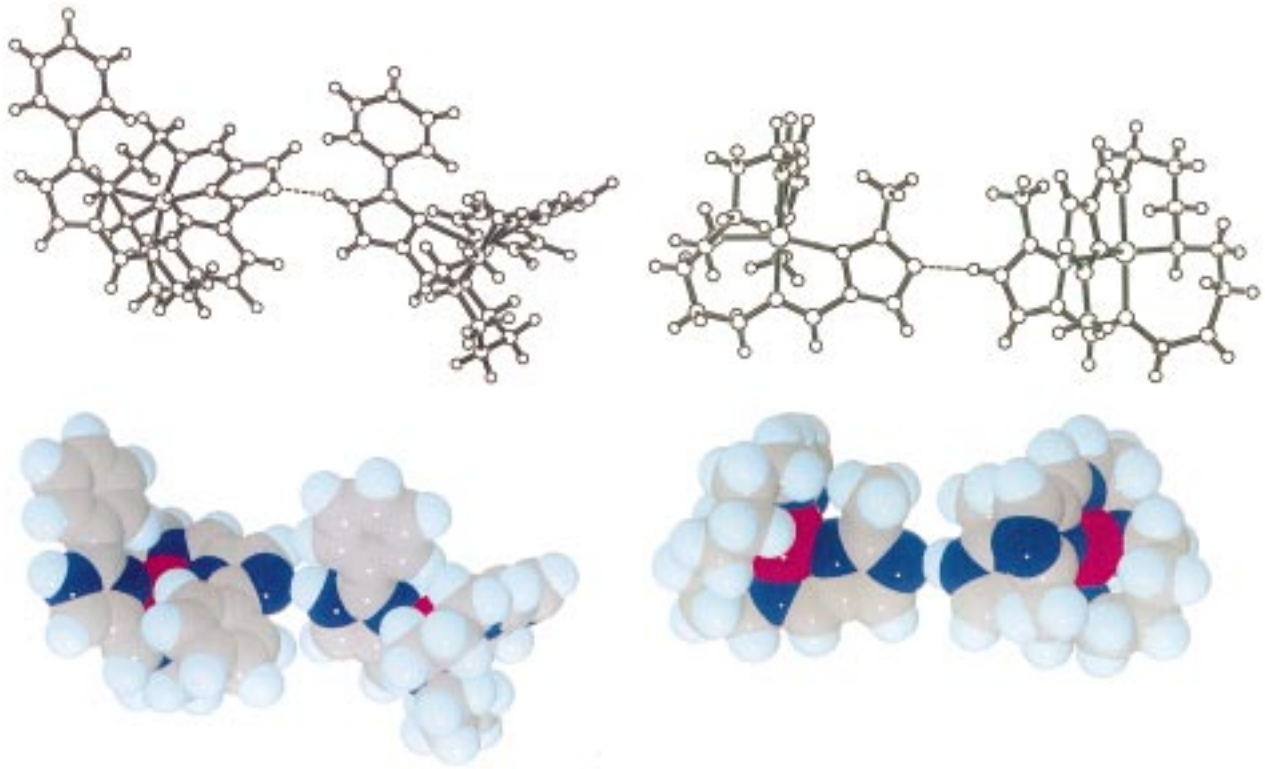

Figure 4. CHARON drawings and space filling representation of the two adjacent molecules linked by the hydrogen bond for **3′** (right) and **4′** (left).

homochiral aggregation of the complex cations is not possible: only complex cations with opposite Δ and Λ chirality are able to interact with each other through hydrogen bonds to yield an extended syndiotactic chain-structure. As a result, the adjacent imidazole and imidazolate rings in **4′** are not in-plane and the Cu−N and N−H bonds are not in-line. Similar heterochiral aggregation was found in the crystal of **5′** with phenyl group. The Cu−N(2) and Cu−N(6) bonds are not in-line, but severely bent toward each other, resulting in a bow-shaped arrangement of the hydrogen-bonded imidazole and imidazolate groups.

The 2-methyl groups of adjacent complex cations in **3′** are oriented in the same direction. As shown by the space filling representation, there is no steric hindrance when small substituents such as methyl groups are oriented in the same direction: the hydrogen-bonded imidazole and imidazolate moieties in **3′** are then roughly in-plane and the Cu−N and N−H bonds are roughly in-line, which is the most suitable to form the N−H···N hydrogen bonds. Considering the N(2)···N(6)* distances and N(2)−H···N(6)* angles in **3′**, **4′**, and **5′**, one can conclude that the alternate aggregation of Δ and Λ enantiomorphs is energetically less favorable in this type of 1D zigzag-chain structure. This allows homochiral aggregation of the complex cations of **3′** into a 1D extended zigzag-chain structure through hydrogen bonding. The present results demonstrate that enantioselective aggregation with either homo- or heterochirality can be controlled by the steric effect of substituents. The relation between the orientation of adjacent substituents and the enantioselective aggregation described above is easily understood by Scheme 2.

We wish to draw attention to the fact that the reported 1D supramolecular structures are not helical- but zigzag-chains. The component building blocks array spirally around the main axis in the case of helical-chains, implying that enantioselectivity is necessarily achieved with homochirality. In the reported 1D zigzag-chains, both Δ and Λ enantiomorphs are present due to the spiral arrangement of the ligand around the main axis of the building complex cation. This axis is roughly perpendicular to the direction of the 1D chains, and therefore aggregation with either homo- or hetero-chirality may be achieved in zigzag-chains.

pH-Dependent Potentiometric Titration and Electronic Spectra. The plots of the proton association number per molecule, *n*, vs pH for **3** and **5** are deposited in Figure S2. In the *n* vs pH plots for **5**, the forward and reverse titration curves show a sigmoid shape and are almost identical. The proton association number *n* decreases from 2 to 0 for the forward titration and increases from 0 to 2 for the reverse titration. These results demonstrate that the protonated (**5**), mono-deprotonated (**5′**), and di-deprotonated (**5″**) species are interconvertible in solution. From the titration curves, the first and second dissociation constants, pK_{d1} and pK_{d2}, were estimated to be 8.5 and 9.4, respectively.

On the other hand, upon titration of **3**, the proton association number *n* did not reach zero ($n = 0.2$) when 2 equiv of NaOH were added to the protonated complex. This suggests that the second imidazole proton does not fully dissociate, and that the amine hydrogen atom may partially dissociate in the higher pH range. The values for the first and second dissociation constants obtained from these titration curves, $pK_{d1} = 9.5$ and $pK_{d2} = 10.6$, are substantially higher than those obtained for **5**. Considering that **3** and **5** include 2-methyl and 2-phenyl imidazoles, respectively, the high dissociation constants in **3** are ascribed to the electron-donating effect of the 2-methyl group of the imidazole moiety.[13]

The pH-dependent electronic spectra of **3** for the forward and reverse procedures are deposited in Figure S3. The spectrum of **3** exhibits a broad band at 681 nm (molar extinction

(13) Smith, R. M.; Martell, A. E. *Critical Stability Constants*; Plenum Press: New York, 1975; Vol. 2.

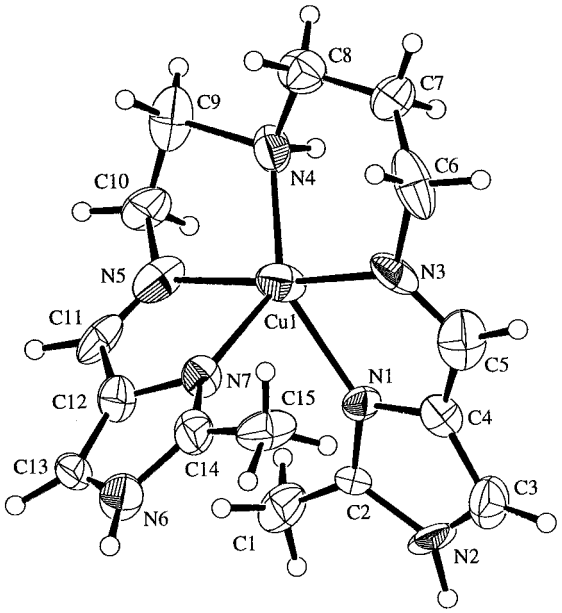

Figure 5. ORTEP drawing of the cation (Δ enantiomorph) for **6** with the atom numbering scheme, showing 30% probability ellipsoids.

coefficient of 129 M^{-1} cm^{-1}) due to a d−d transition. The d−d band showed no change in the maxima and molar extinction coefficient upon titration, indicating that the coordination geometry is retained throughout the deprotonation process. The spectral change exhibits two isosbestic points at 347 and 370 nm. Upon sequential addition of an aqueous NaOH solution, the absorption at ca. 390 nm increased, and conversely the one at ca. 360 nm decreased. The reverse procedure was carried out through sequential addition of an aqueous HCl solution and the spectral change also exhibits two isosbestic points at the same wavelengths, finally reaching the initial spectrum.

Structural Description of 6 and 6′. The crystal structure of **6** consists of a dipositive copper(II) complex cation and two perchlorate counteranions. One of the imidazole nitrogen atoms of the pentadentate ligand involved in the coordination to the complex cation, N(2), is hydrogen-bonded to one perchlorate oxygen atom with a N(2)···O(2) hydrogen bond distance of 2.84(2) Å. The ORTEP drawing of the complex cation including the atom numbering scheme is given in Figure 5. Selected bond distances and angles with their estimated standard deviations are summarized in Table 2. The copper(II) ion assumes a pentacoordinated geometry with two imidazole, two imine, and one amino nitrogen atoms of the pentadentate ligand. The Cu−N bond distances are in the 1.89(2)−2.19(1) Å range, Cu−N(1) being the longer one. Considering that the acyclic pentadentate ligand coordinated to the copper(II) ion is spirally arranged around the N(3)−Cu−N(5) axis, the complex cations are either Δ or Λ enantiomorphs.

The crystals of **6′** consist of an unexpected tetranuclear cyclic complex cation, four perchlorate counteranions, and 16 water molecule as the crystal solvent. The ORTEP drawing of the complex cation with the atom numbering scheme of the unique atoms is shown in Figure 6. The four Cu($HL^{6'}$) units are imidazolate-bridged into a tetranuclear cyclic structure. Selected bond distances and angles with their estimated standard deviations are given in Table 2. The Cu−N(6)* distance corresponding to the imidazolate bridge is 1.972(9) Å (* denotes the symmetry operation of $^3/_4 + y$, $^1/_4 - x$, $^1/_4 - z$). The Cu···Cu distances corresponding to imidazolate bridged and unbridged Cu(II) are 6.086(2) and 8.230(3) Å, respectively. The coordination geometry in **6′** is close to the square pyramid: the N(4), N(5), and N(7) nitrogen atoms of the tetradentate ligand and the N(6)* imidazolate nitrogen atom of the adjacent unit occupy the four equatorial coordination sites with Cu−N distances in the 1.972(9)−2.123(9) Å range. The axial position is occupied by N(1) with a 2.189(9) Å Cu−N distance. The most interesting structural feature of **6′** is the formation of a hexahydropyrimidine ring derived from a rearrangement reaction of the H_2L^6 ligand. The C(5) carbon atom of the resulting $HL^{6'}$ ligand is asymmetric with *R*- or *S*-configuration. In the imidazolate-bridged cyclic-tetranuclear structure, one unit with *R*-configuration bridges to the adjacent unit with *S*-configuration to yield a syndiotactic $(R,S)_2$ cyclic tetramer.

Table 2. Selected Bond Distances (Å) and Angles (deg) of **6** and **6′**

Bond Distances (Å) and Bond Angles (deg) of **6**			
Cu−N(1)	2.19(1)	Cu−N(5)	2.03(2)
Cu−N(3)	1.89(2)	Cu−N(7)	2.10(1)
Cu−N(4)	2.040(8)		
Hydrogen Bond Distances (Å)			
N(2)···O(2)	2.84(2)		
N(1)−Cu−N(3)	78.9(6)	N(3)−Cu−N(5)	175.0(4)
N(1)−Cu−N(4)	126.4(4)	N(3)−Cu−N(7)	100.5(6)
N(1)−Cu−N(5)	105.3(6)	N(4)−Cu−N(5)	73.3(5)
N(1)−Cu−N(7)	89.9(2)	N(4)−Cu−N(7)	140.2(4)
N(3)−Cu−N(4)	101.9(5)	N(5)−Cu−N(7)	82.6(6)
Bond Distances (Å) and Angles (deg) of **6′** [a]			
Cu−N(1)	2.189(9)	Cu−N(6)*	1.972(9)
Cu−N(4)	2.123(9)	Cu−N(7)	2.012(8)
Cu−N(5)	1.975(9)		
N(1)−Cu−N(4)	79.8(3)	N(4)−Cu−N(6)*	96.9(4)
N(1)−Cu−N(5)	106.3(3)	N(4)−Cu−N(7)	162.7(3)
N(1)−Cu−N(6)*	103.7(3)	N(5)−Cu−N(6)*	149.4(4)
N(1)−Cu−N(7)	102.6(3)	N(5)−Cu−N(7)	80.4(4)
N(4)−Cu−N(5)	82.5(4)	N(6)*−Cu−N(7)	99.0(3)

[a] Symmetry operation for **6′** (*): $^3/_4 + y$, $^1/_4 - x$, $^1/_4 - z$.

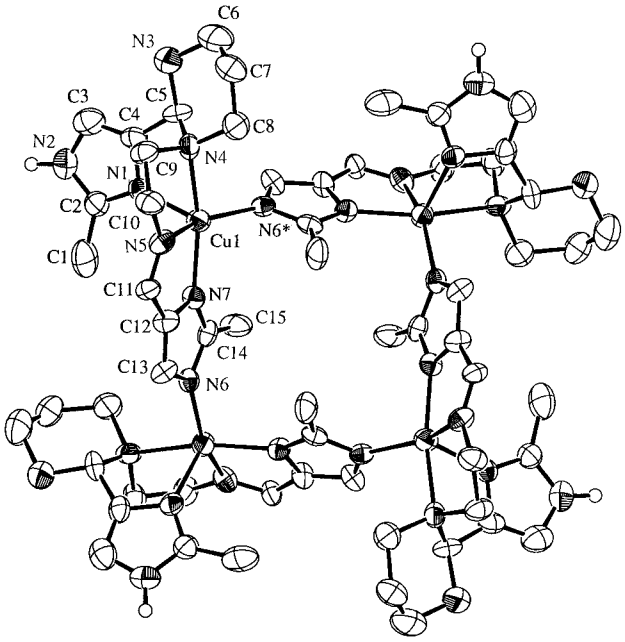

Figure 6. ORTEP drawing of a cyclic-tetranuclear cation of **6′** with the atom numbering scheme, showing 50% probability ellipsoids. Hydrogen atoms excepted for those bound to the asymmetric carbon atom C(5) and the nitrogen atoms are omitted for clarity.

Magnetic Property of the Deprotonated Complex 6′. The magnetic behavior of **6′** is deposited as Figure S4, as χ_A vs T and μ_{eff} vs T plots, where χ_A is the molar magnetic susceptibility per copper, μ_{eff} the effective magnetic moment, and T the absolute temperature. The χ_A vs T curve shows a maximum at

105 K, typical of the magnetic behavior of a tetranuclear cyclic copper(II) complex exhibiting antiferromagnetic interactions.[14] The μ_{eff}/Cu value of 1.61 μ_B at 300 K is smaller than the 1.73 μ_B spin-only value for $S = {}^1/_2$. On lowering the temperature, μ_{eff}/Cu decreases gradually, indicating the operation of an antiferromagnetic interactions. The magnetic susceptibility data were interpreted quantitatively on the basis of the $H = -2J(S_1S_2 + S_2S_3 + S_3S_4 + S_1S_4)$ spin-Hamiltonian for a tetranuclear cyclic spin system,[14] and the corresponding to theoretical magnetic susceptibility derived for $S_1 = S_2 = S_3 = S_4 = {}^1/_2$:

$$\chi_A = (Ng^2\beta^2/2kT)[2 + 5\exp(-2x) + \exp(2x)]/[7 + 5\exp(-2x) + 3\exp(2x) + \exp(4x)] + N\alpha \quad (1)$$

with $x = -J/kT$.

The best-fit parameters, $J = -51.3\ cm^{-1}$ and $g = 2.08$, were obtained by using eq 1 to fit the theoretical variation of the magnetic susceptibility to the experimental data. The J value is compatible with those obtained for imidazolate-bridged dinuclear copper(II) complexes in which the imidazolate group bridges two copper(II) ions at their equatorial sites.[15] The fairly large antiferromagnetic interaction is explained by the $\sigma-\sigma$ superexchange mechanism, since the unpaired electrons of two adjacent copper(II) ions occupy the orbitals lying in the basal coordination planes and can exchange through the imidazolate group.[14,15]

Potentiometric pH Titration of 6. The plots of the proton association number per molecule n vs pH for **6** are obtained by the potentiometric titration measurement. Addition of 2 equiv of NaOH to the solution of the protonated complex yields a proton association number $n = 0.4$. This result suggests that the two imidazole protons are not fully dissociated. The first and second dissociation constants pK_{d1} and pK_{d2} for **6** were estimated to be (pK_{d1}, pK_{d2}) = (9.9, 10.8). These constants are slightly larger than those of **3** and substantially larger than those of **5** and the related copper(II) complex with *N*,*N*′-bis(imidazol-4-ylmethylidene)-1,4-butanediamine ((pK_{d1}, pK_{d2}) = (8.2, 8.8)).[16] The electron-donating 2-methyl group of the imidazole moiety is probably responsible for the increased pK_d values. Coordination of the secondary amine nitrogen atom to copper(II) ion weakens the N−H bond strength of the secondary amine function, increasing the acidity of its hydrogen atom. Therefore, the dissociation constant of the secondary amine hydrogen atom is shifted down to a value closer to the second dissociation constant of the imidazole proton, pK_{d2}. Consequently, when the pH is around 11, deprotonation of the second imidazole and secondary amine function occur competitively.

Ligand Rearrangement and Formation of 6′. Complex **6′** has an imidazolate-bridged tetranuclear cyclic structure and the ligand framework includes a hexahydropyrimidine ring. The deprotonation process of the acyclic pentadentate ligand H_2L^6 induces a rearrangement to the tetradentate ligand $HL^{6'}$. The pH dependent potentiometric titration of **6** suggests that the first deprotonation occurs at one of the imidazoles and the second step competitively occurs at the central secondary amine and the second imidazole sites. A 1:1:2 mixed-solution of the H_2L^6 ligand, copper(II) perchlorate hexahydrate, and sodium hydroxide in water was prepared and its electronic absorption spectrum was periodically recorded at room temperature: the spectrum changed gradually as a function time to resemble that of **6′**. Even after 2 days the spectrum was still changing, indicating that this ligand rearrangement reaction is very slow under these conditions. The possible reaction mechanism (deposited as Figure S5) likely includes the following steps: (1) the secondary amine hydrogen atom is partially dissociated at high pH; (2) the resulting secondary amino anion attacks the imine carbon atom; (3) this attack induces a ligand rearrangement yielding the hexahydropyrimidine ring. A similar ligand rearrangement reaction, also yielding the hexahydro pyrimidine ring, has already been observed in copper(II) complexes containing linear tetramines, and palladium catalyzed reaction of 1,3-propanediamine, azetidine, and allylamine.[17]

Concluding Remarks

The enantioselective self-assembly process of the complexes described in this report can be summarized as follows. (1) The spiral coordination arrangement of the acyclic pentadentate H_2L^n ligands around the copper(II) ion results in an equimolar mixture of Δ and Λ enantiomers. (2) Under proper pH condition, a mono-deprotonated complex cation is generated which includes one imidazole and one imidazolate groups, and functions as a chiral self-complementary (*plerotopic*) double-faced H-bonding recognition unit (*Janus* building block). (3) 1D zigzag-chains result from the self-assembly of these chiral plerotopic Janus complex cations through hydrogen bonds between the imidazole and imidazolate complementary recognition groups. (4) Enantioselective aggregation with either homo- or hetero-chirality can be controlled by the steric effect of substituents: (a) small substituents such as 2-methyl groups allow homo-self-assembly yielding isotactic ...ΔΔΔ... and ...ΛΛΛ... 1D zigzag-chains because they do not impose any steric requirement on the relative orientation of their respective imidazole and imidazolate bearers. Energetically favored almost linear N−H···N bonds may thus result from homochiral aggregation which allows the Cu−N and N−H bonds to be approximately in-line; (b) on the contrary, the steric requirement of bulky substituents such as 2-phenyl groups impose opposite orientations of their respective imidazole and imidazolate bearers. Hetero-self-assembly yielding syndiotactic ...ΔΛΔΛ... zigzag-chains is then the only possibility to achieve enantioselective aggregation of the chiral plerotopic Janus complex cations. Energetically less favored bent N−H···N bonds result from this heterochiral aggregation. (5) Consideration of the different ligands involved in complexes **1′** and **2′** (ref 6) and **3′**−**6′** (this work) show that among the three types of ligand modifications explored, only the 2-substituent of the imidazole ring determines the type of enantioselectivity which controls self-assembly of these chiral plerotopic Janus complex cations. Regardless of (i) the length of the $-(CH_2-)_n$ (n = 2−4) units bridging the central amine to the adjacent imine functions, and (ii) the secondary or tertiary nature of the central amine nitrogen donor of the acyclic pentadentate ligand, nonsterically demanding 2-substituents (H, CH_3) allow the energetically favored homochiral self-assembly, while sterically demanding 2-substituents (C_6H_5) require the energeti-

(14) (a) Carlin, R. L. *Magneto-Structural Correlations in Exchange Coupled Systems*; Willet, R. D., Gatteschi, D., Kahn, O., Eds.; Reidel: Dordrecht, The Nederlands, 1985; p 127. (b) Nakao, Y.; Mori, W.; Okuda, N.; Nakahara, A. *Inorg. Chim. Acta* **1979**, *35*, 1. (c) Costes, J.-P.; Serra, J.-F.; Dahan, F.; Laurent, J.-P. *Inorg. Chem.* **1986**, *25*, 2790.

(15) Carlin, R. L. *Magnetochemistry*; Springer-Verlag: Berlin, Germany, 1986; Chapter 5.

(16) Mimura, M.; Matsuo, T.; Nakashima, T.; Matsumoto, N. *Inorg. Chem.* **1998**, 37, 3553.

(17) (a) Murahashi, S. *Angew. Chem., Int. Ed. Engl.* **1995**, *34*, 2443. (b) Murahashi, S.; Yano, T.; Hino, K. *Tetrahedron Lett.* **1975**, *48*, 4235. (c) Motoda, K.; Aiba, M.; Kokubo, C.; Matsumoto, N.; Okawa, H. *Chem. Lett.* **1995**, 1065.

cally less favored heterochiral self-assembly. (6) Throughout this study, perchlorate ion is used as the counteranion. The effect of the counteranion on the assembly structure and enantioselectivity should be investigated systematically. (7) As shown by the hetero-self-assembly of the tetranuclear cyclic complex cation in **6′**, both the length of the $-(CH_2-)_n$ units bridging the central amine to the adjacent imine functions and the secondary or tertiary nature of the central amine nitrogen donor of the acyclic pentadentate ligand are crucial in promoting the HL^6 ligand rearrangement reaction yielding $HL^{6'}$. The secondary amine function is required to allow formation of the amino anion necessary to attack the imine carbon atom, and both $-(CH_2-)_2$ and $-(CH_2-)_3$ fragments are required to allow formation of the hydropyrimidine ring.

It is revealed how an enantioselective aggregation with homochirality can be achieved within a 1D zigzag-chain. However, the chains with homochiral ΔΔΔ and ΛΛΛ... array alternately to give achiral crystal. If such enantioselective homochiral aggregation could be extended from 1D to 3D system, a spontaneous self-resolution should be achieved automatically. The study along to this line is now in progress in our laboratory.[18]

Experimental Section

General Procedures. All chemicals and solvents used for syntheses were of reagent grade. Reagents used for physical measurements were of spectroscopic grade.

Warning. *Although we used them without any incident, perchlorate salts are potentially explosive and should be handled only in small quantities and with care.*

$[Cu(H_2L^{3-6})](ClO_4)_2\cdot xH_2O$, 3−6. The synthetic procedure used was similar for the four mononuclear precursors. In a representative preparation of **3**, *N*-(3-aminopropyl)-1,4-diaminobutane (0.29 g, 2 mmol) was added to a methanolic solution of 2-methyl-4-formylimidazole (0.44 g, 4 mmol, in 20 mL). The mixture was stirred on a hot plate for 30 min, and the resulting yellow solution was used in the subsequent reaction without isolation of the pentadentate ligand: a methanolic solution of copper(II) chloride dihydrate (0.34 g, 2 mmol, in 20 mL) was added to the ligand solution, and the mixture was stirred for 30 min. A methanolic solution of sodium perchlorate (0.44 g, 4 mmol, in 20 mL) was then added to this reaction mixture. The resulting solution was filtered, and the filtrate was left to stand overnight. The blue microcrystals obtained meanwhile were collected by suction filtration, washed with a small amount of water and methanol, and dried in vacuo. Recrystallization of **3** was performed by slow evaporation of a water/methanol solution.

$[Cu(H_2L^3)](ClO_4)_2$, 3. Yield: 0.7 g (59%). Anal. Calcd for $C_{17}H_{27}N_7O_8Cl_2Cu$: C, 34.50; H, 4.60; N, 16.56. Found: C, 34.30; H, 4.68; N, 16.35. IR (KBr): ν_{N-H}(imidazole), 3150 cm^{-1}; $\nu_{C=N}$(imine), 1630 cm^{-1}; ν_{Cl-O}(perchlorate), 1060−1140 cm^{-1}. UV/vis spectra (H_2O) [λ_{max}/nm (ϵ/M^{-1} cm^{-1})]: 681 (129). Solid (λ_{max}/nm): 720. Λ_M: 200 S cm^2 mol^{-1} in H_2O. Mp: >280 °C.

$[Cu(H_2L^4)](ClO_4)_2$, 4. Attempts to prepare this complex from 2-phenyl-4-formylimidazole (0.34 g, 2 mmol) according to the above procedure, failed to yield a pure solid sample of **4** due to its solubility in commom solvents: the elemental analyses indicated contamination with byproducts.

$[Cu(H_2L^5)](ClO_4)_2\cdot 0.5H_2O$, 5. Yield: 0.9 g (61%). Anal. Calcd for $C_{27}H_{31}N_7O_8Cl_2Cu\cdot 0.5H_2O$: C, 44.72; H, 4.45; N, 13.53. Found: C, 44.85; H, 4.34; N, 13.42. IR (KBr): ν_{N-H}(imidazole), 3125 cm^{-1}; $\nu_{C=N}$(imine), 1640 cm^{-1}; ν_{Cl-O}(perchlorate), 1080−1130 cm^{-1}. UV/vis spectra (H_2O) [λ_{max}/nm (ϵ/M^{-1} cm^{-1})]: 636 (107). Solid (λ_{max}/nm): 598. Λ_M: 187 S cm^2 mol^{-1} in H_2O. Mp: >280 °C.

$[Cu(H_2L^6)](ClO_4)_2$, 6. Yield: 2.2 g (78%). Anal. Calcd for $C_{15}H_{23}N_7O_8Cl_2Cu$: C, 31.95; H, 4.11; N, 17.39. Found: C, 32.21; H, 4.17; N, 17.49. IR (KBr): ν_{N-H}(imidazole), 3100 cm^{-1}; $\nu_{C=N}$(imine), 1638 cm^{-1}; ν_{Cl-O}(perchlorate), 1060−1140 cm^{-1}. UV/vis spectra (H_2O) [λ_{max}/nm (ϵ/M^{-1} cm^{-1})]: 639 (191). Solid (λ_{max}/nm): 639. Λ_M: 203 S cm^2 mol^{-1} in H_2O. Mp: >280 °C. Crystals of **6** suitable for X-ray crystallography were grown by dissolving the complex in the minimum amount of *N*,*N*-dimethylformamide and layering the solution on 2-propanol at room temperature.

$[Cu(HL^{3-5})]ClO_4\cdot xH_2O$, 3′−5′. The synthetic procedure used was similar for **3′**−**5′**. In a representative preparation of **3′**, a methanolic solution of copper(II) perchlorate hexahydrate (0.74 g, 2 mmol, in 30 mL) was added to a 2:1 mixture of 2-methyl-4-formylimidazol (0.44 g, 4 mmol) and *N*-(3-aminopropyl)-1,4-diaminobutane (0.29 g, 2 mmol) in methanol (20 mL). Triethylamine (0.4 g, 4 mmol) was added to the resulting reaction mixture at room temperature. During the addition of triethylamine, the color of the solution changed from blue to green. The reaction mixture was further stirred for 30 min at room temperature and then filtered. The filtrate was left to stand for 1 day. The grayish green microcrystals which deposited meanwhile were filtered off, washed with a small amount of water and methanol, and dried in vacuo.

$[Cu(HL^3)]ClO_4$, 3′. Yield: 0.6 g (61%). Anal. Calcd for $C_{17}H_{26}N_7O_4ClCu$: C, 41.55; H, 5.33; N, 19.95. Found: C, 41.49; H, 5.36; N, 19.84. IR (KBr): ν_{N-H}(imidazole), 3150 cm^{-1}; $\nu_{C=N}$(imine), 1620 and 1640 cm^{-1}; ν_{Cl-O}(perchlorate), 1060−1160 cm^{-1}. UV/vis spectra: solid (λ_{max}/nm): 763. Mp: >280 °C. The crystals were suitable for single-crystal X-ray crystallography.

$[Cu(HL^4)]ClO_4\cdot 0.5H_2O$, 4′. Yield: 1.1 g (87%). Anal. Calcd for $C_{27}H_{30}N_7O_4ClCu\cdot 0.5H_2O$: C, 51.92; H, 5.00; N, 15.70. Found: C, 51.63; H, 5.07; N, 15.51. IR (KBr): ν_{N-H}(imidazole), 3250 cm^{-1}; $\nu_{C=N}$(imine), 1645 cm^{-1}; ν_{Cl-O}(perchlorate), 1080−1140 cm^{-1}. UV/vis spectra: solid (λ_{max}/nm): 599. Mp: >280 °C. These crystals were suitable for single-crystal X-ray crystallography.

$[Cu(HL^5)]ClO_4\cdot H_2O$, 5′. Yield: 1.1 g (86%). Anal. Calcd for $C_{27}H_{30}N_7O_4ClCu\cdot H_2O$: C, 51.18; H, 5.09; N, 15.47. Found: C, 51.72; H, 5.19; N, 15.23. IR (KBr): ν_{N-H}(imidazole), 3025 cm^{-1}; $\nu_{C=N}$(imine), 1645 cm^{-1}; ν_{Cl-O}(perchlorate), 1090−1150 cm^{-1}. UV/vis spectra: solid (λ_{max}/nm): 592. Mp: >280 °C. Crystals suitable for X-ray crystallography were grown by dissolving the complex in dichloromethane/methanol and layering the resulting solution on 2-propanol at room temperature.

$[Cu_4(HL^{6'})_4](ClO_4)_4\cdot 16H_2O$, 6′. Method A. An aqueous solution of sodium hydroxide (40 mg, 1 mmol, 5 mL) was added dropwise to a methanolic solution of complex **6** (282 mg, 0.5 mmol, 10 mL) at room temperature. During the addition, the color of the solution changed from blue to green. The reaction mixture was further stirred for 2 h at room temperature; the resulting green solution was filtered, and the filtrate was left to stand for 1 week. The green crystals deposited meanwhile were collected. The crystals were dried in vacuo and loose the crystal waters. Yield: 10 mg (4%). Anal. Calcd for $C_{15}H_{22}N_7O_4ClCu\cdot 0.25H_2O$: C, 38.50; H, 4.85; N, 20.96. Found: C, 38.74; H, 4.62; N, 20.94. IR (KBr): ν_{N-H}(imidazole), 3250 cm^{-1}; $\nu_{C=N}$(imine), 1620 cm^{-1}; ν_{Cl-O}(perchlorate), 1080−1180 cm^{-1}. UV/vis spectra (H_2O) [λ_{max}/nm (ϵ/M^{-1} cm^{-1})]: 568 (66). Solid (λ_{max}/nm): 699. Λ_{Cu}: 100 S cm^2 mol^{-1} in H_2O. Mp: >280 °C.

Method B. A methanolic solution of copper(II) chloride dihydrate (0.85 g, 5 mmol, 20 mL) was added to a mixed methanolic solution (20 mL) of 2-methyl-4-formylimidazole (1.1 g, 10 mmol) and *N*-(2-aminoethyl)-1,3-propanediamine (0.58 g, 5 mmol), and the reaction mixture was stirred for 30 min. An aqueous solution of sodium hydroxide (0.4 g, 10 mmol, 20 mL) was added to the reaction mixture yielding a color change of the solution from blue to green; the reaction mixture was further stirred for 3 h on a hot plate at 50 °C. A methanolic solution of sodium perchlorate (1.1 g, 10 mmol, 20 mL) was then added, and the reaction mixture was stirred for 10 additional min. The resulting green solution was filtered and the filtrate was left to stand for 1 week. The green crystals which deposited meanwhile were collected by suction filtration, washed with a small amount of methanol, and dried in vacuo. Yield: 1.4 g (60%).

Physical Measurements. Elemental analyses for C, H, and N were performed at the Elemental Analyses Service Center of Kyushu

(18) (a) Mimura, M.; Matsuo, T.; Motoda, Y.; Matsumoto, N.; Nakashima, T.; Kojima, M. *Chem. Lett.* **1998**, 691. (b) Katsuki, I.; Kojima, M.; Matsumoto, N. To be submitted.

Table 3. Crystallographic Data for Copper(II) Complexes[a]

	3′	**4′**	**5′**	**6**	**6′**
empirical formula	$C_{17}H_{26}N_7O_4ClCu$	$C_{27}H_{31}N_7O_{4.5}ClCu$	$C_{27}H_{32}N_7O_5ClCu$	$C_{15}H_{23}N_7O_8Cl_2Cu$	$C_{60}H_{120}N_{28}O_{32}Cl_4Cu_4$
fw	491.44	624.59	633.59	563.84	2141.76
space group	*Pbca* (No. 61)	$P2_1/c$ (No. 14)	$P2_1/c$ (No. 14)	*Cc* (No. 9)	$I4_1/a$ (No. 88)
a, Å	16.245(6)	11.156(3)	13.067(2)	21.800(2)	17.318(3)
b, Å	21.12(1)	20.768(3)	15.166(3)	8.574(1)	17.318(3)
c, Å	12.868(6)	13.065(3)	15.568(2)	16.148(2)	30.432(4)
α, deg	90	90	90	90	90
β, deg	90	114.97(2)	108.138(10)	130.282(4)	90
γ, deg	90	90	90	90	90
V, Å^3	4414(2)	2744(1)	2931.7(7)	2302.7(5)	9126(1)
Z	8	4	4	4	4
ρ_{calcd}, g cm^{-3}	1.479	1.510	1.435	1.626	1.559
μ, cm^{-1}	11.48	9.43	8.85	12.36	11.26
R, R_w	0.052, 0.030	0.069, 0.050	0.067, 0.060	0.045, 0.033	0.083, 0.056

[a] $T = 20 \pm 1$ °C, $\lambda = 0.71063$ Å, $R = \sum||F_o| - |F_c||/\sum|F_o|$, $R_w = [\sum w(|F_o| - |F_c|)^2/\sum w|F_o|^2]^{1/2}$, $w = 1/\sigma(F_o)^2$.

University. Infrared spectra were recorded on a JASCO A-102 spectrophotometer using KBr disks. Electronic absorption spectra and powder reflectance spectra were recorded on a Hitachi U-4000 spectrophotometer. Electrical conductivity measurements were carried out on a Horiba DS-14 conductometer in ca. 1×10^{-3} M aqueous solution. Magnetic susceptibilities were measured with a MPMS5 SQUID susceptometer (Quantum Design Inc.) in the 2−300 K temperature range. The calibrations were made with palladium and $[Ni(en)_3]S_2O_3$ (en = ethylenediamine).[19] Corrections for diamagnetism were applied by using Pascal's constants.[20] Effective magnetic moments were calculated with the equation $\mu_{eff} = 2.828(\chi_A T)^{1/2}$, where χ_A is the magnetic susceptibility per mole of copper ions.

Potentiometric pH Titration. Potentiometric pH-titrations were performed for complexes **3**, **5**, and **6**. All titrations were carried out in a thermostat bath at 25 °C under a 99.9995% N_2 atmosphere. The solvent used in these experiments was extra pure grade water and the resistivity was greater than 18.0 Megohms. The automatic buret Dosimat 665 was supplied from Metrohm Ltd. (Switzerland). The GS-5015c conjugated proton electrode and the IM-40S potentiometer were supplied from TOA Co. Ltd. (Japan). The standard electrode potential (E_0) was first determined by Gran's plot method.[21] 100 mL of 0.15 ionic strength solution containing 0.24 mmol of metal complex and sodium chloride was titrated with a solution containing 0.10 M of NaOH and 0.05 M of NaCl. Immediately after forward titration the resulting solution was titrated back with a solution containing 0.10 M of HCl and 0.05 M of NaCl. All titrations and potential measurements were PC controlled. The electrode potentials were converted into proton concentration scale ($-\log[H^+] = (E_0(mV) - E(mV))/59.15$) and the proton association number, *n*, was calculated by Bjerrum's method[22] for the forward and reverse titrations, respectively.

pH-Dependent Electronic Spectra. pH-Dependent electronic absorption spectra were recorded at room temperature upon sequential addition of 0.1 M aqueous NaOH and HCl solutions for the forward and reverse procedures, respectively. An aqueous solution of the protonated complex (0.24 mmol of the complex in 80 mL of water) was prepared. A spectrum was recorded after each 0.4 mL addition of a 0.1 M NaOH solution, until 2 equiv of NaOH were added. Immediatly after, electronic spectra were recorded for the reverse procedure, following each 0.4 mL addition of a 0.1 M HCl solution to the solution resulting from the forward titration. The spectra were corrected for the volume variation due to the addition of the NaOH and HCl solutions.

X-ray Data Collection, Reduction, and Structure Determination. Each single crystal was mounted on a glass fiber and coated with epoxy resin. All crystallographic measurements were carried out on a Rigaku AFC-7R diffractometer with graphite monochromated Mo Kα radiation ($\lambda = 0.710\,69$ Å) and a 12 kW rotating anode generator. The data were collected at a temperature of 20 ± 1 °C using the $\omega-2\theta$ scan technique to a maximum 2θ value of 50.0° at a scan speed of 8.0−16.0°/min (in omega). The weak reflections ($I < 10.0\sigma(I)$) were rescanned (maximum of 5 scans), and the counts were accumulated to ensure good counting statistics. The intensities of three representative reflections were measured after every 150 reflections. Over the course of the data collection, the standards reflections were monitored and decay corrections were applied through a polynomial correction. An empirical absorption correction based on azimuthal scans of several reflections was applied. The data were also corrected for Lorentz and polarization effects.

The structures were solved by direct methods[23] and expanded using Fourier techniques.[24] The non-hydrogen atoms were anisotropically refined. Hydrogen atoms at their ideal calculated positions were included in the structure factor calculations, but not refined. Full-matrix least-squares refinements ($I > 3.00\sigma(I)$) were employed, where the unweighted and weighted agreement factors of $R = \sum||F_o| - |F_c||/\sum|F_o|$ and $R_w = [\sum w(|F_o| - |F_c|)^2/\sum w|F_o|^2]^{1/2}$ were used. The weighting scheme was based on counting statistics. Plots of $\sum w(|F_o| - |F_c|)^2$ versus $|F_o|$, reflection order in data collection, $\sin\theta/\lambda$ and various classes of indices showed no unusual trends.

The elemental analysis indicated that **4′** contains half a water molecule per formula unit. On the final D-Fourier map, peaks attributable to the water molecule were not located, probably due to the poor quality of the X-ray data and the property of the solvent water molecule. There are two possible space groups for **6**: *Cc* and *C*2/*c*. Considering the unequivalent molecular symmetry and $Z = 4$, we selected *Cc*. Only *Cc* is possible unless disordered.

Neutral atomic scattering factors were taken from Cromer and Waber.[25] Anomalous dispersion effects were included in F_C; the values $\Delta f'$ and $\Delta f''$ were those of Creagh and McAuley.[25] The values for the mass attenuation coefficients were those of Creagh and Hubbel.[26] All calculations were performed using the teXsan crystallographic software

(19) Lindoy, L. F.; Katovic, V.; Busch, D. H. *J. Chem. Educ.* **1972**, *49*, 117.
(20) (a) Boudreaux, E. A.; Mulay, L. N. *Theory and Applications of Molecular Paramagnetism*; Wiley: New York, 1976; p 491. (b) Earnshaw, A. *Introduction to Magnetochemistry*; Academic Press: New York, 1968.
(21) Gran, G. *Analyst* **1952**, *77*, 661.
(22) Beck, M. T.; Nagypal, I. *Chemistry of Complex Equilibria*; Wiley: New York, 1990; p 44.
(23) (a) Fan H-F. *SAPI91, Structure Analysis Programs with Intelligent Control*; Rigaku Corporation: Tokyo, Japan, 1991. (b) Debaerdemaeker, T.; Germain, G.; Main, P.; Refaat, L. S.; Tate, C.; Woolfson, M. M. *MULTAN88*; 1988.
(24) Beurskens, P. T.; Admiraal, G.; Beurskens, G.; Bosman, W. P.; Garcia-Granda, S.; Gould, R. O.; Smits, J. M. M.; Smykalla, C. *DIRDIF92: The DIRDIF Program System*; Technical Report of the Crystallography Laboratory, University of Nijmegen: The Netherlands, 1992.
(25) (a) Creagh, D. C.; McAuley, W. J. *International Tables for Crystallography*; Wilson, A. J. C., Ed.; Kluwer Academic Publishers: Boston, MA, 1992; Vol. C, Table 4.2.6.8, pp 219−222. (b) Cromer, D. T.; Waber, J. T. *International Tables for X-ray Crystallography*; The Kynoch Press: Birmingham, England, 1974; Vol. IV, Table 2.2A.
(26) Creagh, D. C.; Hubbel, J. H. *International Tables for Crystallography*; Wilson, A. J. C., Ed.; Kluwer Academic Publishers: Boston, MA, 1992; Vol. C, Table 4.2.4.3, pp 200−206.

package of the Molecular Structure Corporation.[27] Crystal data and details of the structure determination are summarized in Table 3.

Acknowledgment. This work was supported by Monbusho International Scientific Research Program (No. 10044089 "Joint Research") and by a Grant-in-Aid for Scientific Research on Priority Area (No. 10149101 "Metal-assembled Complexes").

(27) *teXsan: Crystal Structure Analysis Package*; Molecular Structure Corporation: The Woodlands, TX, 1985 and 1992.

Supporting Information Available: Five X-ray crystallographic files, in CIF format, are available only on the Internet. Five figures are deposited as supplementary figures (Figures S1−S5). This material is available free of charge via the Internet at http://pubs.acs.org.

IC9813260